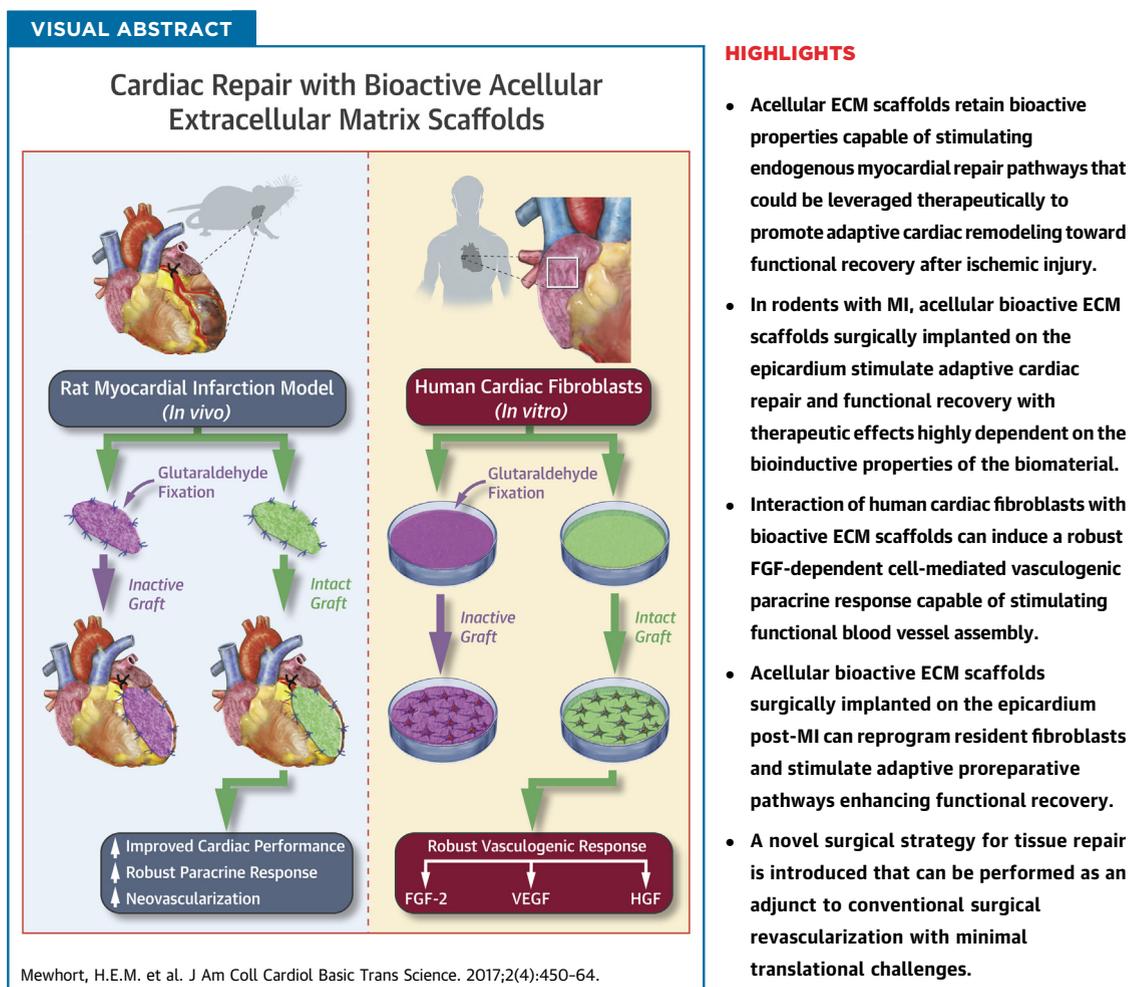**PRECLINICAL RESEARCH**

# Bioactive Extracellular Matrix Scaffold Promotes Adaptive Cardiac Remodeling and Repair

Holly E.M. Mewhort, MD, PhD,[a] Daniyil A. Svystonyuk, BSc,[a] Jeannine D. Turnbull, BSc,[a] Guoqi Teng, PhD,[a]
Darrell D. Belke, PhD,[a] David G. Guzzardi, BSc,[a] Daniel S. Park, BSc,[a] Sean Kang, BSc,[a]
Morley D. Hollenberg, MD, PhD,[b] Paul W.M. Fedak, MD, PhD[a]

## VISUAL ABSTRACT



Cardiac Repair with Bioactive Acellular Extracellular Matrix Scaffolds

Mewhort, H.E.M. et al. J Am Coll Cardiol Basic Trans Science. 2017;2(4):450–64.

### HIGHLIGHTS

- Acellular ECM scaffolds retain bioactive properties capable of stimulating endogenous myocardial repair pathways that could be leveraged therapeutically to promote adaptive cardiac remodeling toward functional recovery after ischemic injury.

- In rodents with MI, acellular bioactive ECM scaffolds surgically implanted on the epicardium stimulate adaptive cardiac repair and functional recovery with therapeutic effects highly dependent on the bioinductive properties of the biomaterial.

- Interaction of human cardiac fibroblasts with bioactive ECM scaffolds can induce a robust FGF-dependent cell-mediated vasculogenic paracrine response capable of stimulating functional blood vessel assembly.

- Acellular bioactive ECM scaffolds surgically implanted on the epicardium post-MI can reprogram resident fibroblasts and stimulate adaptive proreparative pathways enhancing functional recovery.

- A novel surgical strategy for tissue repair is introduced that can be performed as an adjunct to conventional surgical revascularization with minimal translational challenges.

From the [a]Section of Cardiac Surgery, Department of Cardiac Sciences, Cumming School of Medicine, Libin Cardiovascular
Institute of Alberta, University of Calgary, Calgary, Alberta, Canada; and the [b]Department of Physiology and Pharmacology,
Department of Medicine, Cumming School of Medicine, Snyder Institute for Chronic Disease, University of Calgary, Calgary,
Alberta, Canada. Project funding was provided to Dr. Fedak by Heart and Stroke Foundation of Canada. Salary support for
Dr. Mewhort was provided by Alberta Innovates Health Solutions. Salary support for Mr. Svystonyuk was provided by Alberta

## ABBREVIATIONS AND ACRONYMS

**ANOVA** = analysis of variance

**ECM** = extracellular matrix

**EF** = ejection fraction

**EMT** = epithelial-to-mesenchymal transition

**FGF** = fibroblast growth factor

**HGF** = hepatocyte growth factor

**HUVEC** = human umbilical vein endothelial cell

**LV** = left ventricle

**MI** = myocardial infarction

**SIS-ECM** = small intestinal submucosal extracellular matrix

**VEGF** = vascular endothelial growth factor

### SUMMARY

Structural cardiac remodeling after ischemic injury can induce a transition to heart failure from progressive loss of cardiac function. Cellular regenerative therapies are promising but face significant translational hurdles. Tissue extracellular matrix (ECM) holds the necessary environmental cues to stimulate cell-based endogenous myocardial repair pathways and promote adaptive remodeling toward functional recovery. Heart epicardium has emerged as an important anatomic niche for endogenous repair pathways including vasculogenesis and cardiogenesis. We show that acellular ECM scaffolds surgically implanted on the epicardium following myocardial infarction (MI) can attenuate structural cardiac remodeling and improve functional recovery. We assessed the efficacy of this strategy on post-MI functional recovery by comparing intact bioactive scaffolds with biologically inactivated ECM scaffolds. We confirm that bioactive properties within the acellular ECM biomaterial are essential for the observed functional benefits. We show that interaction of human cardiac fibroblasts with bioactive ECM can induce a robust cell-mediated vasculogenic paracrine response capable of functional blood vessel assembly. Fibroblast growth factor-2 is uncovered as a critical regulator of this novel bioinductive effect. Acellular bioactive ECM scaffolds surgically implanted on the epicardium post-MI can reprogram resident fibroblasts and stimulate adaptive pro-reparative pathways enhancing functional recovery. We introduce a novel surgical strategy for tissue repair that can be performed as an adjunct to conventional surgical revascularization with minimal translational challenges.  (J Am Coll Cardiol Basic Trans Science 2017;2:450–64)
© 2017 The Authors. Published by Elsevier on behalf of the American College of Cardiology Foundation. This is an open access article under the CC BY-NC-ND license (http://creativecommons.org/licenses/by-nc-nd/4.0/).

Despite innovative treatment advances, the burden of cardiovascular disease remains high [1]. Ischemic cardiovascular injury is prevalent and the resultant damage is often irreversible with a poor prognosis despite optimal contemporary therapies [2]. Thus, the ensuing chronic structural remodeling process leads to irreversible heart failure due to myocardial fibrosis, wall thinning, and progressive left ventricular (LV) dilation [3]. Myocardial revascularization alone is beneficial but is incapable of completely preventing progressive remodeling, loss of systolic function, and the threatening transition to clinical heart failure.

Tissue-derived extracellular matrix (ECM) provides a critical microenvironment that supports cell survival, function, and adaptive tissue repair processes. The ECM maintains a passive structural scaffold with biomechanical effects on cells. In addition, ECM provides a reservoir of bioactive growth factors and matricellular proteins that enable bioinductive effects that influence cell phenotype and behavior [4,5]. Dysregulation of the ECM after ischemic injury can mediate maladaptive structural remodeling and induce a loss of function [6]. Restoring ECM integrity after ischemic injury may therefore be capable of promoting adaptive healing and functional recovery.

The epicardium is a key anatomic compartment that coordinates critical regenerative processes and pathways during neonatal heart development [7]. Recently, the regenerative capacity of the epicardium was highlighted in the adult mammalian heart [8]. The epicardium can thus be seen as an optimal location for introducing factors that may improve the myocardial regenerative process. We therefore hypothesized that ECM applied to the epicardium can serve as a source of such factors that can promote tissue regeneration.

In keeping with this proposed therapeutic role of ECM, we found that in clinically relevant animal models of human cardiac disease the epicardial implantation of acellular tissue-derived ECM scaffolds can attenuate maladaptive structural cardiac remodeling and promote functional recovery [9,10]. The present study was designed to uncover the mechanism(s) underlying this therapeutic outcome that was not identified in our previous work [9,10].

Our hypothesis was that the bioactive components retained in the ECM scaffold are essential for the observed functional benefits. Using a rat coronary ligation infarct model, we therefore compared the impact of intact tissue-derived ECM scaffolds with ECM that had been treated either by glutaraldehyde cross-linking or extraction with guanidine hydrochloride to inactivate any ECM-adsorbed bioactive constituents. We found that the interaction of human cardiac fibroblasts with intact (but not inactivated) ECM can induce a robust vasculogenic paracrine response capable of promoting functional blood vessel assembly. Basic fibroblast growth factor (FGF)-2 is shown to be a critical regulator of this novel bioinductive effect.

## METHODS

**ACELLULAR ECM SCAFFOLD.** A commercially available intact porcine small intestinal submucosal extracellular matrix (SIS-ECM) (CorMatrix-ECM, CorMatrix Cardiovascular Inc., Roswell, Georgia) was used. The SIS-ECM scaffold was rehydrated by soaking it in phosphate-buffered saline (Lonza, Walkersville, Maryland). Inactivation of the ECM scaffold was achieved by either glutaraldehyde cross-linking or by dissociating and denaturing ECM-adsorbed constituents with 4 mol/l guanidine hydrochloride. Glutaraldehyde-inactivated ECM scaffold was prepared by soaking it in 0.6% glutaraldehyde at 4°C for 24 h. Bioinactivated ECM scaffold was then transferred to 0.2% glutaraldehyde and stored at 4°C until use. Denaturing ECM and dissociating adsorbed factors was achieved by soaking in 4 mol/l guanidine hydrochloride at room temperature overnight. Before use, the cross-linked and denatured SIS-ECM preparations were extensively washed with isotonic phosphate-buffered saline to remove the inactivating reagents.

**RAT MYOCARDIAL INFARCTION MODEL.** Animal handling and myocardial infarction (MI) was performed as previously described (9). In brief, animals were anesthetized and maintained with isoflurane for the duration of the surgical procedure. Using left anterolateral thoracotomy, the left anterior descending artery was ligated. The incision was reapproximated and animals were recovered.

**SURGICAL IMPLANTATION OF ECM SCAFFOLD.** Infarcted animals were randomly assigned to 1 of 3 groups: 1) intact ECM scaffold implantation; 2) inactivated ECM scaffold implantation; or 3) sham procedure. The treatment procedure was performed 3 weeks post-MI. The heart was exposed by left anterolateral thoracotomy 1 intercostal space caudal to the previous incision. The infarcted region was identified visually. Animals had either intact or inactivated ECM scaffolds sewn onto the epicardial surface of the infarct using a continuous 7-0 polypropylene suture. Animals randomized to the sham group underwent a similar suture technique performed without securing an ECM scaffold. The incision was reapproximated and the animals were recovered. Analgesia, antibiotic prophylaxis, and preoperative fluids were administered as described herein.

**ECHOCARDIOGRAPHY.** Echocardiographic evaluation was performed 2 weeks post-MI (as a baseline before treatment) and 14 weeks post-MI. All echocardiograms were performed under isoflurane inhalational anesthesia in the dorsal decubitus position and recorded using an Esaote MyLab30 Gold Cardiovascular Ultrasound system (Canadian Veterinary Imaging, Georgetown, Ontario, Canada). Animals with an ejection fraction (EF) >50% were not randomized.

**CARDIAC PRESSURE-VOLUME LOOP ANALYSIS.** Hemodynamic parameters were further assessed using a pressure-volume loop system at 14 weeks post-MI. A 2-F conductance catheter (SPR-838 or SPR849, Millar Instruments, Houston, Texas) was inserted into the LV via the right carotid artery. LV pressure and volume data were collected and analyzed as previously described using ADInstruments software (Colorado Springs, Colorado) (11).

**PARACRINE RESPONSE OF CARDIAC FIBROBLASTS TO INTACT ECM SCAFFOLD.** Human cardiac fibroblasts were isolated as previously described (Supplemental Methods, Supplemental Table 1). A total of 100,000 cardiac fibroblasts were seeded onto circular (10-mm diameter) ECM scaffolds (or cell culture plastic as a control) and incubated in serum-free Iscove modified Dulbecco medium for 24 h at 37°C in 5% $CO_2$. The resulting conditioned media was collected, labeled alpha-numerically, and sent for blinded analysis to quantify the concentration of FGF-2, hepatocyte growth factor (HGF), and vascular endothelial growth factor (VEGF) by multiplex analysis (Eve Technologies, Calgary, Alberta, Canada). FGF-2 was blocked using 1 μmol/l of FGF-2 receptor inhibitor (PD 173074, Sigma-Aldrich, St. Louis, Missouri). The resulting conditioned media was collected as described herein and the concentration of FGF-2, HGF, and VEGF was quantified by multiplex analysis.

**HUMAN UMBILICAL VEIN ENDOTHELIAL CELL VASCULOGENESIS ASSAY.** In a 24-well, 1-cm diameter multidish tray (Corning, Corning, New York), 300 μl of growth factor–reduced Matrigel (Corning) was

polymerized for 15 min at 37°C in 5% $CO_2$. Human umbilical vein endothelial cells (HUVECs) (BD Biosciences, San Jose, California) were seeded at 60,000 cells per well. Intact or guanidine hydrochloride-inactivated ECM scaffolds were floated above the cell-matrix constructs in 500 µl of serum-free Medium 200 (Thermo Fisher Scientific, Waltham, Massachusetts) for 6 h at 37°C in 5% $CO_2$. Guanidine hydrochloride-inactivated scaffolds were used instead of glutaraldehyde-inactivated scaffolds to avoid cross-linking of the Matrigel substrate by residual glutaraldehyde, thereby avoiding a false negative result. Cell-matrix constructs were fixed in 4% paraformaldehyde and imaged using light microscopy (Zeiss, Jena, Germany). Each data point was averaged from 5 random images that were blindly analyzed using ImageJ Angiogenesis Analyzer (National Institutes of Health, Bethesda, Maryland) for length of tubes formed, length of branches formed, number of junctions formed, and number of nodes formed.

**STATISTICAL ANALYSIS.** All data are expressed as mean ± SD of at least 3 independent experiments. For in vitro experiments using human cells, we assumed a normally distributed population and performed a parametric analysis. Prism 6.0h (GraphPad Software Inc., San Diego, California) statistical software was used for all statistical analysis. Where appropriate, data were analyzed by unpaired Student *t* test when comparing 2 samples and analysis of variance (ANOVA) was used when comparing multiple samples. Post hoc comparisons were analyzed with Bonferroni test. Samples that violated the equal variance assumption of the Student *t* test were analyzed with Welch correction. We considered p values <0.05 to be significant.

## RESULTS

To determine the influence of bioactive properties on structural and functional benefits of ECM scaffold implantation, we implanted ECM scaffolds on the epicardium of rats 3 weeks after coronary ligation induced MI. We then quantified the impact of the different scaffolds on post-MI structural remodeling and functional recovery at 14 weeks post-MI or 11 weeks post-ECM implantation. Using 2 independent methods to assess cardiac performance, we found that the bioactive properties of the intact ECM scaffolds were necessary to enhance post-MI functional recovery.

**INTACT ECM SCAFFOLD IMPROVES POST-MI CARDIAC PERFORMANCE.** EF was assessed by echocardiography at baseline (2 weeks post-MI) and 14 weeks post-MI. A progressive decline in EF was observed in both inactivated ECM scaffold- and sham-treated animals (decrease in EF: 5.1 ± 8.0% vs. 8.0 ± 5.1%) as compared to intact ECM scaffold-treated animals, which showed improvement in EF over time (increase in EF: 6.8 ± 6.9%) (**Figure 1A**). Pressure-volume loop analysis was performed at 14 weeks post-MI, and EF was compared between groups. Intact ECM scaffold-treated animals had significantly higher EF as compared to both inactivated ECM scaffold- and sham-treated animals (42.6 ± 7.6% vs. 33.6 ± 9.0% vs. 28.7 ± 13.2%, respectively; p = 0.0017) (**Figure 1B**).

Load-independent indices of cardiac systolic performance were also measured by pressure-volume loop analysis at 14 weeks post-MI. The end-systolic pressure-volume relationship showed improved contractility in intact ECM scaffold-treated animals as compared to inactivated ECM scaffold- and sham-treated animals (0.9 ± 0.3 mm Hg/µl vs. 0.6 ± 0.3 mm Hg/µl vs. 0.5 ± 0.3 mm Hg/µl, respectively; p = 0.0007) (**Figure 1C**). Pre-load recruitable stroke work was significantly higher in intact ECM scaffold-treated animals as compared to inactivated ECM scaffold- and sham-treated animals (79.0 ± 15.6 mm Hg/µl vs. 51.2 ± 27.6 mm Hg/µl vs. 50.2 ± 23.1 mm Hg/µl, respectively; p = 0.0038) (**Figure 1D**). Finally, the change in LV pressure over time divided by the LV end-diastolic volume demonstrated improved cardiac performance in intact ECM scaffold-treated animals as compared to both inactivated ECM scaffold- and sham-treated animals (26.5 ± 5.6 mm Hg·µl/s vs. 17.8 ± 6.7 mm Hg·µl/s vs. 20.3 ± 4.4 mm Hg·µl/s, respectively; p = 0.0013) (**Figure 1E**). These data confirm that intact ECM that retains its bioactive properties is essential to inducing functional recovery post-MI. The biomechanical effects of ECM scaffold therapy may be less critical to inducing functional recovery.

**INTACT ECM SCAFFOLD ATTENUATES MALADAPTIVE STRUCTURAL REMODELING.** We further explored effects on structural chamber remodeling. LV end-diastolic volumes were assessed by pressure-volume loop analysis. LV volume in inactivated ECM scaffolds- and sham-treated animals at 14 weeks post-MI was greater than age and body mass for comparable uninjured hearts (341.2 ± 48.4 µl vs. 373.7 ± 78.8 µl vs. 231.6 ± 63.5 µl, respectively; p = 0.0001) (**Figures 2A and 2C**), suggesting progressive LV dilatation. LV end-diastolic volumes were, however, comparatively smaller in intact ECM scaffold-treated animals (298.0 ± 53.4 µl; p = 0.0001), indicating attenuation of progressive LV structural remodeling after intact ECM scaffold treatment.

**FIGURE 1** Intact ECM Scaffold Improves Post-MI Cardiac Performance
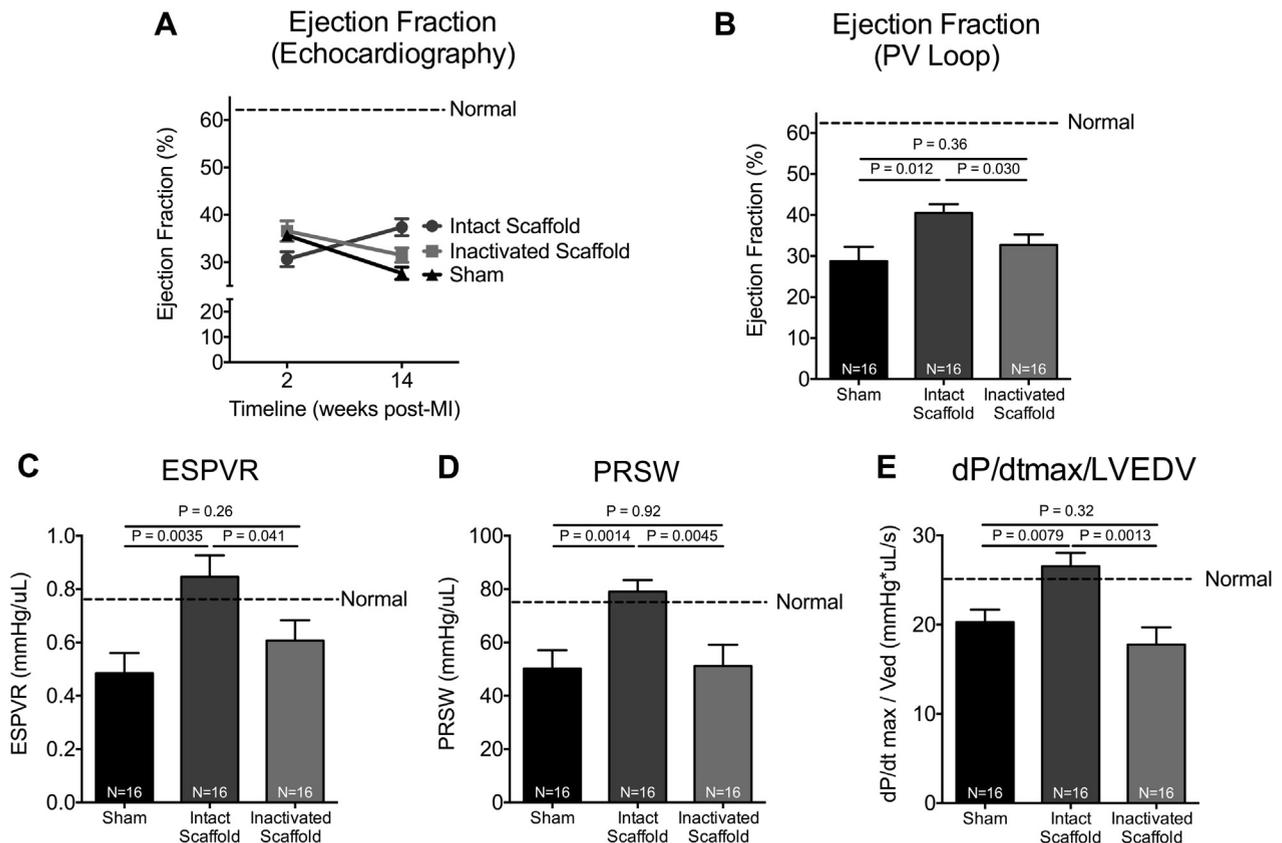
**(A)** Ejection fraction of sham-treated (n = 16) and intact (n = 16) and glutaraldehyde-inactivated (n = 16) extracellular matrix (ECM) scaffold–treated animals as measured by serial echocardiography. Significant effects were observed for time (p = 0.048) but not group (p = 0.38). Effect interaction (group × time) was significant (p = 0.0001) (repeated measures 2-way analysis of variance [ANOVA]). **(B)** Ejection fraction was also analyzed by pressure-volume loop analysis 14 weeks post-myocardial infarction (MI) (1-way ANOVA). Load-independent markers of cardiac performance including end-systolic pressure-volume relationship (ESPVR) **(C)**, pre-load recruitable stroke work (PRSW) **(D)**, and maximum pressure change divided by left ventricular end-diastolic volume (dP/dt max/LVEDV) **(E)** measured by pressure-volume (PV) loop at 14 weeks post-MI in sham-treated (n = 16) and intact (n = 16) and glutaraldehyde-inactivated (n = 16) ECM scaffold–treated animals (1-way ANOVA).

Thickness of the infarcted anterior myocardial wall was also measured by serial echocardiography. Wall thickness was increased in both intact and inactivated ECM scaffold-treated animals as compared to sham-treated animals at 14 weeks post-MI (0.9 ± 0.3 mm vs. 0.8 ± 0.3 mm vs. 0.6 ± 0.1 mm, respectively; p = 0.034) (Figures 2B and 2D). Postmortem examination of explanted hearts demonstrated that anterior wall thickness in intact ECM scaffold-treated animals was the result of a tissue thickening of the myocardium versus maladaptive encapsulation of the ECM scaffold, which was consistently observed in inactivated glutaraldehyde-fixed ECM scaffold-treated animals (Figure 2B). Given that wall thickness was not different between the treatment groups, we

suggest that wall thickening did not contribute to the observed functional and structural benefits. However, these data suggest that the intact ECM was biocompatible and more consistent with adaptive tissue formation and recovery.

**ECM SCAFFOLD DOES NOT INCREASE LV STIFFNESS.** Implanting ECM scaffolds, a form of fibrous tissue, on the surface of the heart could have detrimental effects on chamber compliance with negative consequences over time. Accordingly, we assessed and compared LV stiffness after ECM scaffold implantation. The end-diastolic pressure-volume relationship, an index of LV stiffness, was measured by pressure-volume loop analysis at 14 weeks post-MI. LV
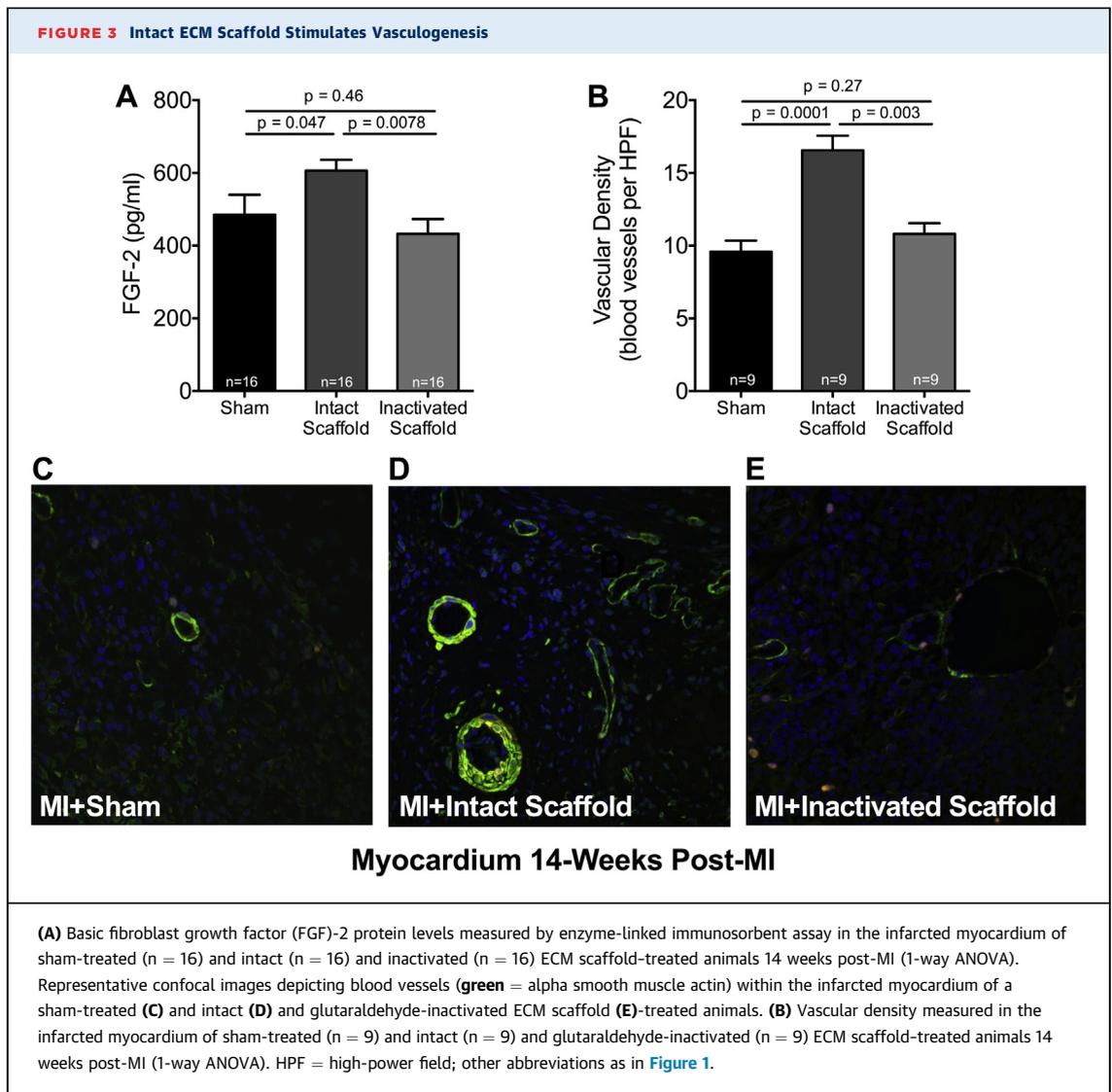
**FIGURE 2** Intact ECM Scaffold Attenuates Maladaptive Structural Remodeling
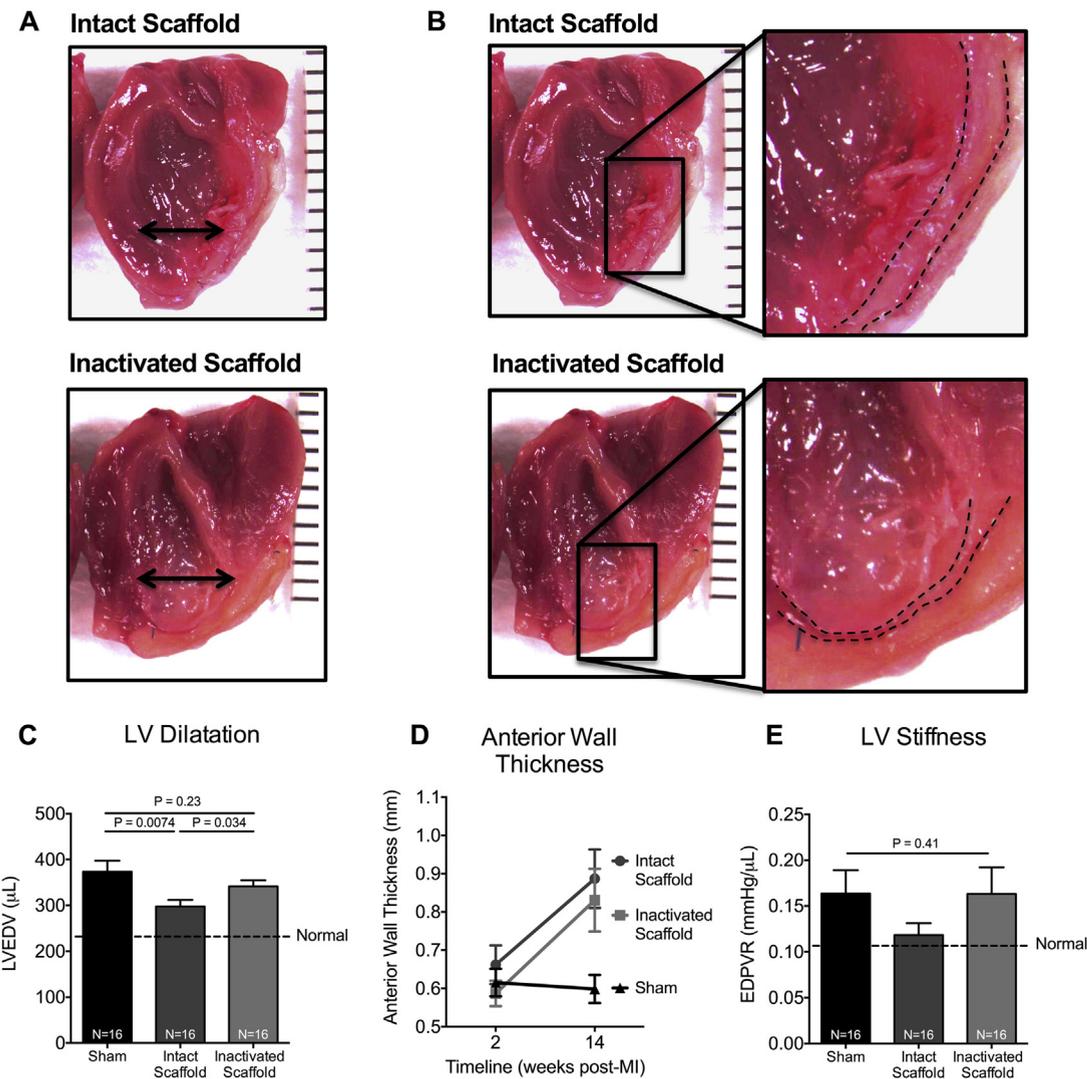
(A) Representative images of LV divided long axis depicting relative LV volumes and geometry. (B) Representative images of the treated infarcted anterior LV wall (**dashed line** indicates the endocardial and epicardial borders of the LV wall) depicting anterior wall thickness and ECM scaffold. (C) LVEDV measured by PV loop analysis in sham-treated (n = 16) and intact (n = 16) and glutaraldehyde-inactivated (n = 16) ECM scaffold-treated animals 14 weeks post-MI (1-way ANOVA). Infarcted LV anterior wall thickness measured by echocardiography in sham-treated (n = 16) and intact (n = 16) and glutaraldehyde-inactivated (n = 16) ECM scaffold-treated animals. (D) Significant differences were observed for effects of time (p = 0.0012), group (p = 0.034), and interaction (group × time, p = 0.034) (repeated measures 2-way ANOVA). (E) LV stiffness indicated by end-diastolic pressure-volume relationship (EDPVR) measured by PV loop analysis in sham-treated (n = 16) and intact- (n = 16) and glutaraldehyde-inactivated (n = 16) ECM scaffold-treated animals 14 weeks post-MI (1-way ANOVA). Abbreviations as in **Figure 1**.

stiffness was similar between intact and inactivated ECM scaffolds-treated as compared to sham-treated animals (end-diastolic pressure-volume relationship: 0.1 ± 0.1 mm Hg/µl vs. 0.2 ± 0.1 mm Hg/µl vs. 0.2 ± 0.1 mm Hg/µl, respectively; p = 0.41) (**Figure 2E**). Interestingly, a trend toward increased LV compliance

(less stiff) was observed in the intact ECM scaffold-treated animals, reflecting absolute values closer to that of a noninfarcted heart. These data confirm that intact ECM scaffolds do not negatively alter LV compliance and may perhaps improve myocardial biomechanics after ischemic injury. These data also

**FIGURE 3**   Intact ECM Scaffold Stimulates Vasculogenesis

**(A)** Basic fibroblast growth factor (FGF)-2 protein levels measured by enzyme-linked immunosorbent assay in the infarcted myocardium of sham-treated (n = 16) and intact (n = 16) and inactivated (n = 16) ECM scaffold–treated animals 14 weeks post-MI (1-way ANOVA). Representative confocal images depicting blood vessels (**green** = alpha smooth muscle actin) within the infarcted myocardium of a sham-treated **(C)** and intact **(D)** and glutaraldehyde-inactivated ECM scaffold **(E)**-treated animals. **(B)** Vascular density measured in the infarcted myocardium of sham-treated (n = 9) and intact (n = 9) and glutaraldehyde-inactivated (n = 9) ECM scaffold–treated animals 14 weeks post-MI (1-way ANOVA). HPF = high-power field; other abbreviations as in **Figure 1**.

suggest that reductions in LV size were not a maladaptive side effect of increasing regional myocardial stiffness.

**INTACT ECM SCAFFOLD STIMULATES VASCULOGENESIS.** To explore a paracrine-mediated mechanism of the observed structural and functional benefits, protein levels of FGF-2 in the infarcted myocardium of sham-treated and intact and inactivated-treated animals were measured by enzyme-linked immunosorbent assay. A significant increase in FGF-2 expression was observed in intact ECM scaffold–treated animals as compared to inactivated ECM scaffold–treated animals 14 weeks post-MI ($606.4 \pm 107.8$ pg/ml vs. $432.5 \pm 157.4$ pg/ml; $p = 0.0081$) (**Figure 3A**). Importantly, these data show that intact ECM scaffolds can

induce a unique provasculogenic paracrine response in the infarcted myocardium in vivo.

Given the increase in paracrine mediators of vasculogenesis, we next assessed regional myocardial vascularity. The increase in vasculogenic growth factor expression in the infarcted myocardium of intact ECM scaffold–treated animals was matched by a significant increase in vascularity as measured by fluorescence immunohistochemistry. Vascular density of the infarcted myocardium of intact ECM scaffold–treated animals 14 weeks post-MI demonstrated a marked increase in vascularity as compared to both inactivated ECM scaffold- and sham-treated animals ($16.6 \pm 3.0$ vs. $10.8 \pm 2.2$ vs. $9.6 \pm 2.3$ blood vessels per high power field, respectively; $p = 0.0001$) (**Figures 3B to 3E**). These observations suggest
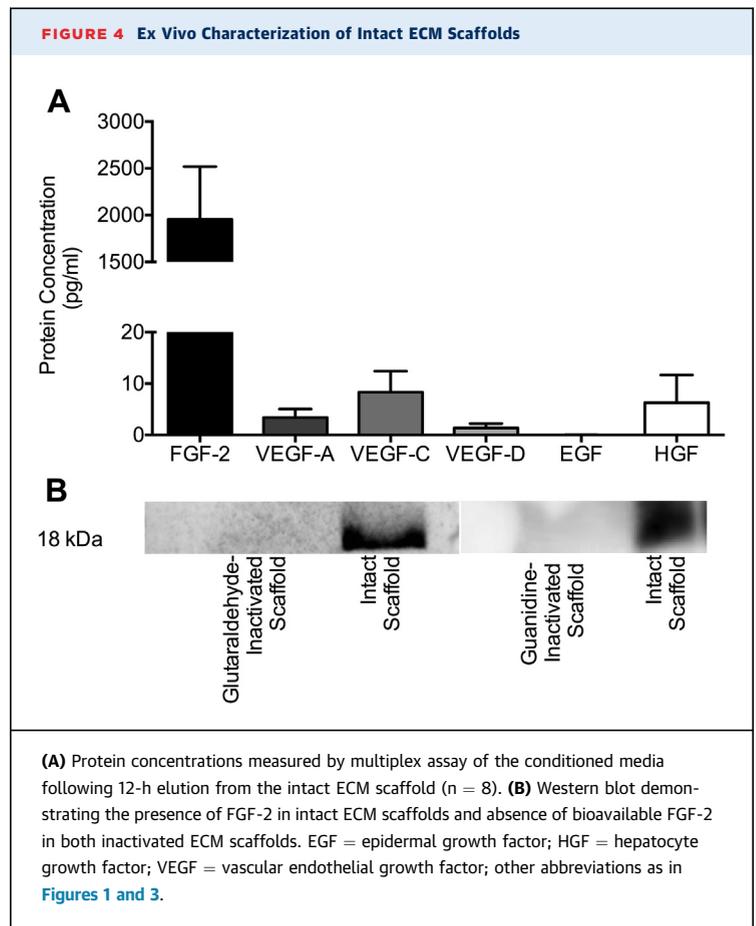
that intact bioactive ECM scaffolds induced myocardial vasculogenesis in association with enhanced paracrine mediators as late as 14 weeks after implantation.

**EX VIVO CHARACTERIZATION OF INTACT ECM SCAFFOLDS.** Given the enhanced production of myocardial FGF-2 observed and the knowledge that intact ECM scaffolds retain endogenous growth factors, we next characterized the ex vivo elution profile of growth factors from the intact ECM scaffold. Multiplex assay analysis of conditioned media following a 12-h incubation of intact ECM scaffolds in serum-free media at 37°C demonstrated elution of high concentrations of FGF-2 (1,954.0 ± 563.9 pg/ml). VEGF isoforms A, C, and D also eluted from the ECM scaffolds with concentrations lower than FGF-2 (3.4 ± 1.7 pg/ml, 8.3 ± 4.1 pg/ml, and 1.4 ± 0.8 pg/ml, respectively) (**Figure 4A**). These data suggest that the intact ECM scaffold used in the study is rich in FGF-2, which is capable of being liberated from the biomaterial under passive conditions.

To biologically inactivate and abolish any bioactive properties within the ECM scaffolds, glutaraldehyde-fixation and guanidine-neutralization were performed. We then measured endogenous FGF-2 in the intact ECM scaffolds as compared to glutaraldehyde-inactivated and guanidine-inactivated ECM scaffolds by Western blot. The presence of FGF-2 in the intact ECM scaffold and the lack of FGF-2 bioavailability in both glutaraldehyde- and guanidine-inactivated ECM scaffolds was confirmed (**Figure 4B**). These observations indirectly support, but do not confirm, the role of scaffold FGF-2 in mediating functional benefits after implantation in the injured heart.

**PROVASCULOGENIC PARACRINE RESPONSE TO INTACT ECM SCAFFOLD.** Cardiac fibroblasts are abundant and active in infarcted myocardium following ischemic injury. To assess for a bioinductive effect of the ECM scaffold on host cells, we characterized the paracrine response of human cardiac fibroblasts when in contact with the intact ECM scaffold. Conditioned media from human cardiac fibroblasts cultured on plastic, intact ECM scaffold, and glutaraldehyde-inactivated ECM scaffold were analyzed by multiplex assays and compared.

Human cardiac fibroblasts exposed to intact ECM scaffolds increased production of FGF-2, VEGF, and HGF as compared to inactivated ECM scaffolds where the paracrine response was profoundly muted (FGF-2: 7.1 ± 4.1- vs. 2.6 ± 1.4-fold change, respectively; p = 0.043; VEGF: 2.8 ± 2.2- vs. 0.8 ± 0.6-fold change, respectively; p = 0.030; HGF: 8.7 ± 7.0- vs. 1.1 ± 0.7-fold change, respectively; p = 0.045) (**Figures 5A**



**FIGURE 4  Ex Vivo Characterization of Intact ECM Scaffolds**

**(A)** Protein concentrations measured by multiplex assay of the conditioned media following 12-h elution from the intact ECM scaffold (n = 8). **(B)** Western blot demonstrating the presence of FGF-2 in intact ECM scaffolds and absence of bioavailable FGF-2 in both inactivated ECM scaffolds. EGF = epidermal growth factor; HGF = hepatocyte growth factor; VEGF = vascular endothelial growth factor; other abbreviations as in **Figures 1 and 3**.

**to 5C**). Importantly, these unique observations suggest that cell-ECM scaffold interactions further stimulate sustained paracrine mediator production that may be capable of inducing vasculogenesis.

To determine whether the elution of endogenous FGF-2 from the intact ECM scaffold is an important regulator of increased vasculogenic growth factors as observed, we cultured human cardiac fibroblasts on intact ECM scaffolds in the presence of an FGF-2 receptor inhibitor (PD 173074, Sigma-Aldrich). FGF-2 receptor blockade attenuated cardiac fibroblast production of FGF-2, VEGF, and HGF when compared with cardiac fibroblasts treated with intact ECM scaffold in the absence of FGF-2 receptor blockade (FGF-2: 2,914.0 ± 359.5 pg/ml vs. 2,299.0 ± 256.1 pg/ml, respectively; p = 0.073; VEGF: 4,168.0 ± 1,709.0 pg/ml vs. 1,364.0 ± 698.9 pg/ml, respectively; p = 0.058; HGF: 1,164.0 ± 141.4 pg/ml vs. 228.0 ± 142.1 pg/ml, respectively; p = 0.001) (**Figures 5D to 5F**). These data suggest that endogenous FGF-2 eluted from the intact ECM scaffold is, in part, responsible for observed bioinductive effects on human cardiac fibroblasts.

**FIGURE 5    Provasculogenic Paracrine Response to Intact ECM Scaffold**
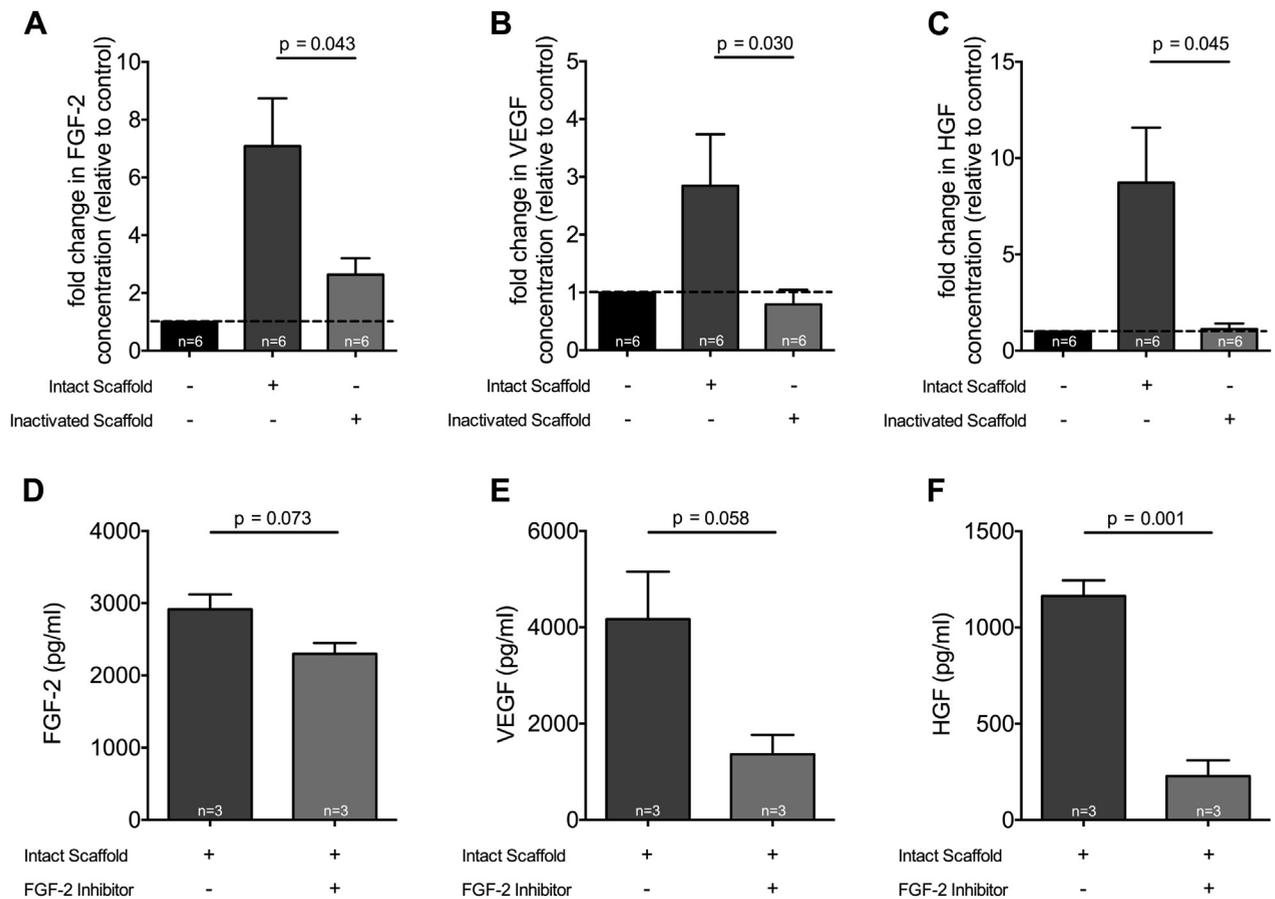
Fold change relative to control in FGF-2 **(A)**, VEGF **(B)**, and HGF **(C)** concentrations measured by multiplex assays of the conditioned media of human cardiac fibroblasts grown on plastic (n = 6), intact ECM scaffold (n = 6), or glutaraldehyde-inactivated ECM scaffold (n = 6; Student *t* test). FGF-2 **(D)**, VEGF **(E)**, and HGF **(F)** concentrations measured by multiplex assays of the conditioned media of human cardiac fibroblasts grown on plastic (n = 3), intact ECM scaffold (n = 3), or intact ECM scaffold in the presence of 1 μmol/l of FGF-2 receptor inhibitor PD 173074 (n = 3; Student *t* test). Abbreviations as in **Figures 1, 3, and 4**.

**INTACT ECM SCAFFOLD SUPPORTS BLOOD VESSEL ASSEMBLY.** We evaluated the in vitro vasculogenic potential of ECM scaffold treatment to show that increased vascularity could be a direct result of bioactive properties of ECM scaffolds. To that end, HUVEC were seeded onto growth factor-reduced Matrigel with intact ECM scaffold or guanidine-inactivated ECM scaffolds and parameters of in vitro blood vessel assembly were quantified. Intact ECM scaffold treatment of HUVEC resulted in increased vascular network formation as represented by an increase in total tubule length (26.3 ± 2.8 mm vs. 22.2 ± 1.6 mm vs. 22.0 ± 2.9 mm, respectively; p = 0.009) (**Figure 6D**), total tubule branch length (19.2 ± 3.1 mm vs. 13.2 ± 2.0 mm vs. 13.7 ± 2.5 mm, respectively; p = 0.002) (**Figure 6E**), number of nodes (366.2 ± 67.1

vs. 236.6 ± 42.5 vs. 242.4 ± 46.1, respectively; p = 0.002) (**Figure 6F**), and number of junctions (106.9 ± 19.2 vs. 69.9 ± 12.9 vs. 71.7 ± 13.6, respectively; p = 0.002) (**Figure 6G**) compared with both control and inactivated ECM scaffold-treated cells.

These data confirm that intact bioactive ECM releases paracrine mediators that are capable of inducing new blood vessel formation in adjacent cells.

## DISCUSSION

We confirm that acellular ECM scaffolds surgically implanted on the epicardial surface attenuates post-MI structural cardiac remodeling and improves functional recovery. For the first time, we show that bioactive properties are essential for the observed

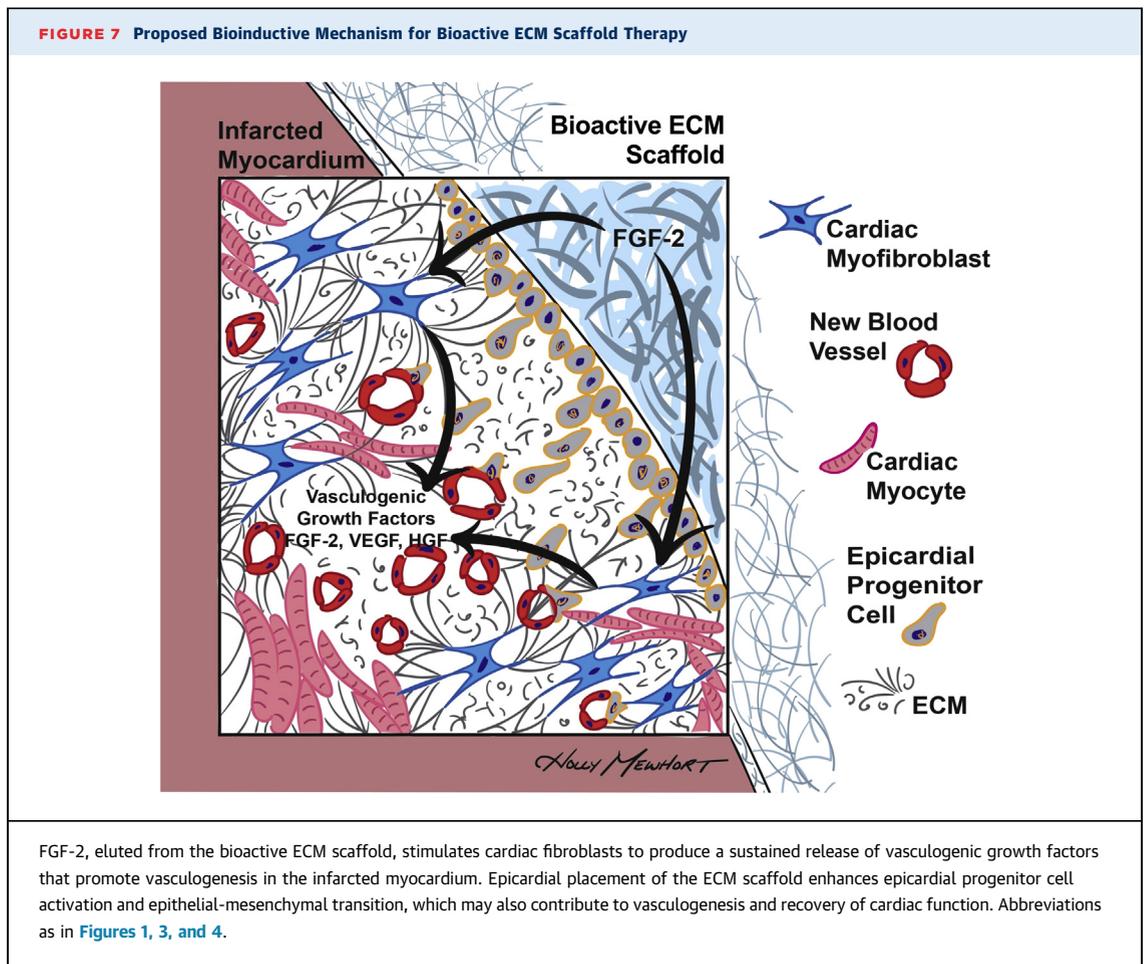**FIGURE 6  Intact ECM Scaffold Supports Blood Vessel Assembly**
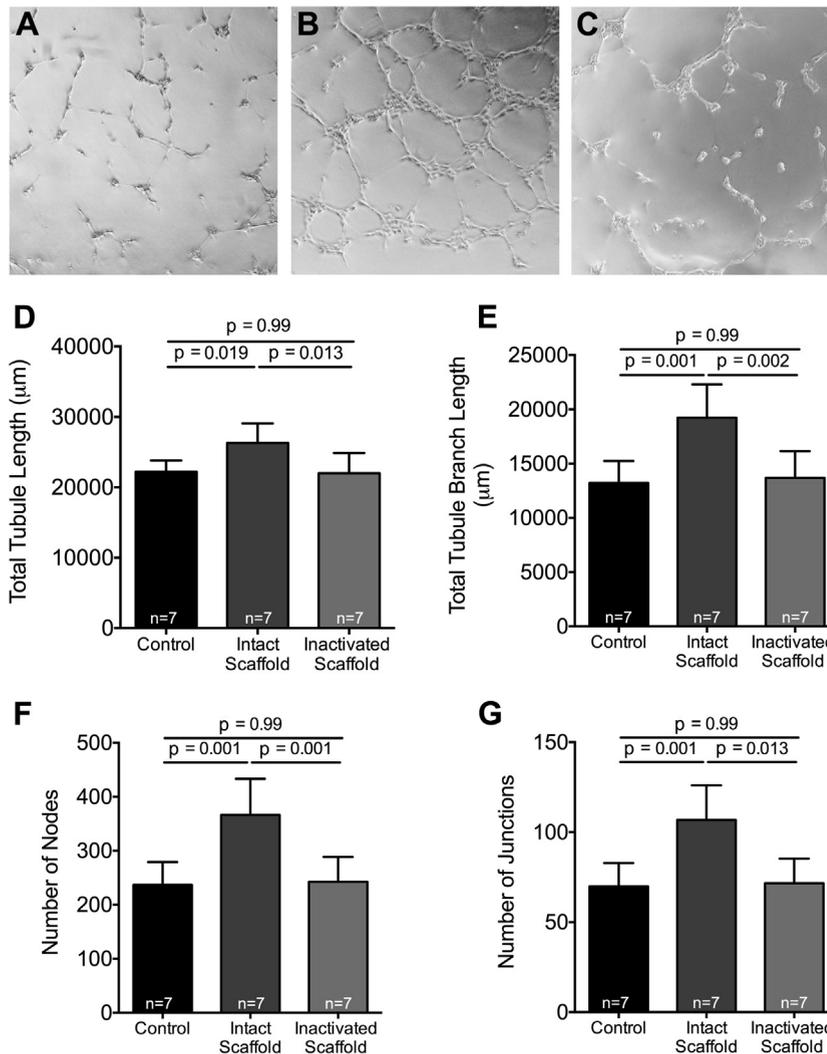
Representative images of the human umbilical vein endothelial cell angiogenesis assays performed with no scaffold **(A)**, intact ECM scaffold **(B)**, and guanidine-inactivated ECM scaffolds **(C)**. Total tubule length **(D)**, total tubule branch length **(E)**, number of nodes **(F)**, and number of junctions **(G)** measured in human umbilical vein endothelial cell angiogenesis assays performed with serum-free media (n = 7), intact ECM scaffold (n = 7), and guanidine-inactivated ECM scaffold (n = 7; 1-way ANOVA). Abbreviations as in **Figure 1**.

functional benefits. FGF-2 is found as a critical mediator of its bioinductive effects on host cells and tissues. Whereas FGF-2 is shown to be released from the biomaterial itself, the sustained myocardial FGF-2 elevations (at 14 weeks) and resultant paracrine-mediated vasculogenesis observed are better explained as a consequence of ongoing host cell-scaffold interactions (**Figure 7**). We provide novel data to support that human cardiac fibroblasts when in contact with intact bioactive ECM scaffolds will produce vasculogenic paracrine factors, including

FGF-2, which we show are capable of stimulating blood vessel assembly. These mechanistic data may have important implications for the development and validation of emerging therapeutic strategies using acellular biomaterials to improve outcomes after ischemic myocardial injury.

**LEVERAGING BIOACTIVE ECM AS A THERAPEUTIC STRATEGY.** ECM serves as a dynamic microenvironment for surrounding cells by way of embedded growth factors, matricellular proteins, and cell-ECM

**FIGURE 7    Proposed Bioinductive Mechanism for Bioactive ECM Scaffold Therapy**

FGF-2, eluted from the bioactive ECM scaffold, stimulates cardiac fibroblasts to produce a sustained release of vasculogenic growth factors that promote vasculogenesis in the infarcted myocardium. Epicardial placement of the ECM scaffold enhances epicardial progenitor cell activation and epithelial-mesenchymal transition, which may also contribute to vasculogenesis and recovery of cardiac function. Abbreviations as in Figures 1, 3, and 4.

receptors. After decellularization from tissues, acellular ECM scaffolds can retain bioinductive properties due to bioactive constituents such as FGF-2 that remain sequestered in the native ECM material (12). ECM is recognized as essential for endogenous tissue repair and cell regeneration mechanisms (13). Cardiac fibroblasts, the most abundant cell type in the heart, can synthesize ECM components and other paracrine factors that can modulate myocardial tissue (14). Accordingly, the activities of fibroblasts within their ECM microenvironment influences cardiac homeostasis (15). Although fibroblasts are typically associated with fibrous scar tissue production following injury, recent studies implicate these cells as key regulators of regenerative processes such as angiogenesis (16). Newman et al. (16) demonstrated that fibroblasts produce a paracrine milieu that significantly enhanced endothelial tube formation and does so more effectively than exogenous growth factor treatments alone. Similarly, we believe that our data highlight an unappreciated interaction of cardiac fibroblasts with bioactive ECM scaffolds that shifts the cells toward a proangiogenic phenotype that supports blood vessel formation.

## ACELLULAR ECM BIOMATERIALS FOR USE IN CARDIAC REPAIR.

We and others are exploring innovative strategies for cardiac repair using novel acellular biomaterials (9,17,18). We used a natural scaffold biomaterial derived from porcine SIS-ECM for this study. Badylak et al. (19) repaired the ventricular free wall of animals with SIS-ECM and noted adaptive tissue formation. CorMatrix-ECM is a SIS-ECM that is commercially available and approved by the U.S. Food and Drug Administration for intracardiac applications. It has been applied in numerous human cardiac surgery procedures (20). CorMatrix-ECM has been shown to retain its native ECM architecture, matricellular protein composition, and multiple cell signaling proteins, rendering it potentially bioactive (21,22). Despite its xenogeneic nature, in vivo studies suggest a good immune tolerance of SIS-ECM (22).

Whereas we show bioactive effects of SIS-ECM, cardiac-derived ECM scaffolds may hold additional benefits to trigger cardiac-specific repair. D'Amore et al. (18) created a biosynthetic patch with porcine myocardial ECM and showed bioactive effects and functional benefits consistent with our in vivo observations. Although epicardial-based biomechanical restraint strategies have been clinically unsuccessful, bioinjectable materials may provide a new avenue for this emerging therapeutic strategy. An injectable alginate hydrogel has shown promising results when combined with standard treatment as opposed to standard treatment alone in the AUGMENT-HF (A Randomized, Controlled Study to Evaluate Algisyl-LVR as a Method of Left Ventricular Augmentation for Heart Failure) clinical study (23). Injectable biomaterials that leverage bioactive properties of ECM in combination with passive biomechanical effects may further enhance post-MI functional recovery (24).

### BIOINDUCTIVE VERSUS BIOMECHANICAL EFFECTS OF ECM SCAFFOLDS. The precise mechanisms underlying the observed functional benefits have important implications for the clinical translation of ECM scaffold therapy. If bioactive ECM scaffold effects are a result of passive epicardial restraint from its biomechanical properties, then a similarly noncompliant and clinically applicable material such as Dacron graft materials could provide comparative benefits. Previous clinical trials exploring passive epicardial mechanical restraint, such as PEERLESS-HF (Prospective Evaluation of Elastic Restraint to Lessen the Effects of Heart Failure), failed to show significant clinical benefits (25). Importantly, we show that the benefits of ECM scaffold therapy are dependent on the bioactive properties of the material itself. The provasculogenic properties of FGF-2, which we confirm are eluted from ECM scaffold, are well established (26). We extended our mechanistic observations in vitro where we show that human cardiac fibroblasts secreted high concentrations of provasculogenic growth factors (FGF-2, VEGF, and HGF) as a result of a specific interaction with intact bioactive ECM scaffolds. The interaction between human cardiac fibroblasts and intact bioactive ECM scaffolds induced an approximate 10-fold increase in HGF expression. Beyond its vasculogenic properties, HGF has a known cardioprotective role that helps maintain cardiomyocyte survival and reduce fibrosis in the infarcted myocardium (27,28). We also show that the paracrine properties of the ECM scaffold supported the organization of human endothelial cells into

vascular networks, highlighting that the scaffolds are indeed bioactive.

The functional benefits of ECM scaffold therapy draw many parallels to experimental cell-based therapies but with fewer translational hurdles (29). Cell therapy results in attenuation of LV remodeling and improved cardiac function, despite a transient survival of transplanted cells in the host tissue (30). These benefits are believed to be mediated by short-term paracrine effects (31,32). To that end, the bioinductive capacity observed with acellular ECM scaffolds could mimic the paracrine benefits of cell therapy but with more sustained effects. Whereas the acellular ECM scaffold was rich in bioavailable FGF-2, the finite amount cannot persist indefinitely once the reservoir in the biomaterial is depleted after implantation in vivo. Interestingly, we note myocardial FGF-2 was elevated as late as 14 weeks after implantation. We provide novel and important data that suggest that sustained effects of ECM scaffold implantation are likely the result of cell-scaffold interactions and not simply persistent elution from the biomaterial. The interaction of host cells with the implanted biomaterial may be a critical feature for sustained paracrine effects as compared to injected cell therapy without biomaterials. Interestingly, acellular scaffolds can be further enhanced with exogenous growth factors or progenitor cell treatments to optimize therapeutic effects (9,17).

Although neovascularization, as shown in our study, has been extensively studied in improving cardiac function post-MI, we acknowledge the importance of exploring additional mechanisms (Supplemental Figure 1). A recent study demonstrated that acellular ECM scaffolds mobilized endogenous progenitor cells and shifted the inflammatory profile of injured skeletal muscle toward an enhanced reparative state (33). Further exploration of the immunomodulatory effects of ECM scaffold therapy on the post-MI heart is warranted. An improved understanding of the specific bioinductive effects of ECM scaffolds may help inform efforts to optimize the bioactive potential of this platform technology to influence adaptive cardiac repair.

### EPICARDIUM AS A THERAPEUTIC TARGET FOR BIOMATERIAL IMPLANTS. Following ischemic injury, epicardial progenitor cells are reactivated and capable of contributing to myocardial repair through an epithelial-to-mesenchymal transition (EMT) pathway (34). Epicardial thickening in response to ischemic injury has been shown to act as a source of paracrine factors that condition the underlying

myocardium for repair (35). FGF-2 has been implicated as a key paracrine factor in these epicardial repair mechanisms (34). Artificial induction of EMT has been shown to improve post-MI cardiac remodeling (34). In light of these observations, targeting the epicardial space with bioactive ECM scaffold therapy may facilitate and promote endogenous repair.

Several markers of epicardial progenitor cell activation and EMT have been identified including nuclear translocation of β-catenin (35). We demonstrate an increase in nuclear translocation of β-catenin in the infarcted myocardium of animals treated with bioactive ECM scaffolds (Supplemental Figure 2). Although further mechanistic studies of epicardial progenitor cells and EMT pathways are warranted, our results show preliminary evidence that the epicardium may be primed with intact bioactive ECM scaffolds for enhanced therapeutic benefit. Other cardioprotective effects such as mitigation of fibrosis and cardiogenesis are possible, but they were not specifically explored in this study.

**STUDY LIMITATIONS.** Glutaraldehyde fixation is the gold standard method for rendering xenogeneic materials biologically inactive before surgical implantation. However, glutaraldehyde fixation may alter its biomechanical properties, and these properties were not directly measured in our study. In addition, glutaraldehyde elution from the inactivated ECM scaffold could potentially influence the underlying infarcted myocardium. We noted evidence of cell toxicity when glutaraldehyde-inactivated ECM scaffolds were applied in our HUVEC vasculogenesis assay, prompting the use of a guanidine-inactivation strategy. The in vivo application of ECM scaffolds inactivated via other methods (including guanidine neutralization) is being investigated.

Furthermore, although we show that FGF-2 released from intact ECM scaffolds is necessary for the fibroblasts to assume a proangiogenic state, we suspect that this phenotypic shift is likely due to a combination of both the paracrine effects of the biomaterial as well as the cell-biomaterial interactions. Additionally, it is well supported in the published reports that FGF-2 is capable of inducing cell proliferation, and we believe it is possible that our biomaterial-released FGF-2 may be doing something similar (36). Although cell proliferation was not directly assessed in this study, we believe that the proliferation of a proangiogenic fibroblast phenotype

may assist in the observed neovascularization of intact ECM scaffold-treated animals. Specifically, the vasculogenic paracrine profile and ECM remodeling characteristics of these fibroblasts may be necessary for vascular cell recruitment, organization, and stabilization. Our future work aims to better characterize the role of fibroblast-ECM scaffold interactions.

## CONCLUSIONS

Coronary artery bypass graft surgery presents a unique opportunity to directly treat the injured region that initiates, coordinates, and maintains the maladaptive signals for the heart to remodel despite successful revascularization. Bioactive ECM scaffold implantations can be performed as an adjunct to surgical revascularization with minimal risk and cost. Bioactive ECM scaffold treatment directed to the epicardium may induce sustained microscopic myocardial vessel formation that in combination with concomitant macroscopic epicardial vessel grafting, may work synergistically to enhance perfusion within areas at risk and recruit and restore damaged myocardium. Approximately 5% to 10% of patients admitted with an acute coronary syndrome receive coronary artery bypass graft surgery early after injury (37). Over 1.5 million patients are admitted with acute coronary syndromes each year in North America. Clinical application of acellular bioactive ECM scaffold therapy (CorMatrix-ECM) in post-MI patients is currently being evaluated by our translational research team (phase 1, Epicardial Infarct Repair Using CorMatrix-ECM: Clinical Feasibility Study [EIR]; NCT02887768). With further clinical validation, bioactive ECM therapy could become a standard of care for patients after ischemic injury who require surgical revascularization.

**ADDRESS FOR CORRESPONDENCE:** Dr. Paul W.M. Fedak, Section of Cardiac Surgery, Department of Cardiac Sciences, Cumming School of Medicine, Libin Cardiovascular Institute of Alberta, University of Calgary, C880, 1403-29 Street NW, Calgary, Alberta T2N 2T9, Canada. E-mail: paul.fedak@gmail.com.

## PERSPECTIVES

**COMPETENCY IN MEDICAL KNOWLEDGE:** This study shows that bioinductive properties are necessary for acellular ECM scaffolds to stimulate endogenous cardiac repair mechanisms post-MI. Epicardial-targeted acellular ECM scaffold implantation has minimal translational challenges and is a promising therapeutic strategy to restore functional recovery after ischemic injury.

**TRANSLATIONAL OUTLOOK:** This study used porcine-derived decellularized ECM that is FDA-approved for clinical use. Surgical application of this acellular ECM scaffold is feasible early after infarction as an adjunct to surgical revascularization. The scaffold can be placed as an epicardial patch targeted to the region of myocardial injury. We are currently evaluating this novel surgical strategy to enhance tissue repair in a Phase 1 clinical trial (NCT02887768).

### REFERENCES

**1.** Mozaffarian D, Benjamin EJ, Go AS, et al. Executive summary: heart disease and stroke statistics—2016 update: a report from the American Heart Association. Circulation 2016;133:447-54.

**2.** Fedak PW, Verma S, Weisel RD, Li RK. Cardiac remodeling and failure from molecules to man (part II). Cardiovasc Pathol 2005;14:49-60.

**3.** Velagaleti RS, Pencina MJ, Murabito JM, et al. Long-term trends in the incidence of heart failure after myocardial infarction. Circulation 2008;118:2057-62.

**4.** Lukashev ME, Werb Z. ECM signalling: orchestrating cell behaviour and misbehaviour. Trends Cell Biol 1998;8:437-41.

**5.** Faulk DM, Johnson SA, Zhang L, Badylak SF. Role of the extracellular matrix in whole organ engineering. J Cell Physiol 2014;229:984-9.

**6.** Baicu CF, Stroud JD, Livesay VA, et al. Changes in extracellular collagen matrix alter myocardial systolic performance. Am J Physiol Heart Circ Physiol 2003;284:H122-32.

**7.** Cai CL, Martin JC, Sun Y, et al. A myocardial lineage derives from Tbx18 epicardial cells. Nature 2008;454:104-8.

**8.** Wei K, Serpooshan V, Hurtado C, et al. Epicardial FSTL1 reconstitution regenerates the adult mammalian heart. Nature 2015;525:479-85.

**9.** Mewhort HE, Turnbull JD, Meijndert HC, Ngu JM, Fedak PW. Epicardial infarct repair with basic fibroblast growth factor-enhanced CorMatrix-ECM biomaterial attenuates postischemic cardiac remodeling. J Thorac Cardiovasc Surg 2014;147:1650-9.

**10.** Mewhort HE, Turnbull JD, Satriano A, et al. Epicardial infarct repair with bioinductive extracellular matrix promotes vasculogenesis and myocardial recovery. J Heart Lung Transplant 2016;35:661-70.

**11.** Pacher P, Nagayama T, Mukhopadhyay P, Bátkai S, Kass DA. Measurement of cardiac function using pressure-volume conductance catheter technique in mice and rats. Nat Protoc 2008;3:1422-34.

**12.** Voytik-Harbin SL, Brightman AO, Kraine MR, Waisner B, Badylak SF. Identification of extractable growth factors from small intestinal submucosa. J Cell Biochem 1997;67:478-91.

**13.** Bayomy AF, Bauer M, Qiu Y, Liao R. Regeneration in heart disease—is ECM the key? Life Sci 2012;91:823-7.

**14.** Baudino TA, Carver W, Giles W, Borg TK. Cardiac fibroblasts: friend or foe? Am J Physiol Heart Circ Physiol 2006;291:H1015-26.

**15.** Rosso F, Giordano A, Barbarisi M, Barbarisi A. From Cell-ECM interactions to tissue engineering. J Cell Physiol 2004;199:174-80.

**16.** Newman AC, Nakatsu MN, Chou W, Gershon PD, Hughes CC. The requirement for fibroblasts in angiogenesis: fibroblast-derived matrix proteins are essential for endothelial cell lumen formation. Mol Biol Cell 2011;22:3791-800.

**17.** Perea-Gil I, Prat-Vidal C, Bayes-Genis A. In vivo experience with natural scaffolds for myocardial infarction: the times they are a-changin'. Stem Cell Res Ther 2015;6:248.

**18.** D'Amore A, Yoshizumi T, Luketich SK, et al. Bilayered polyurethane—extracellular matrix cardiac patch improves ischemic ventricular wall remodeling in a rat model. Biomaterials 2016;107:1-14.

**19.** Badylak S, Obermiller J, Geddes L, Matheny R. Extracellular matrix for myocardial repair. Heart Surg Forum 2003;6:E20-6.

**20.** Mosala Nezhad Z, Poncelet A, de Kerchove L, Gianello P, Fervaille C, El Khoury G. Small intestinal submucosa extracellular matrix (CorMatrix®) in cardiovascular surgery: a systematic review. Interact Cardiovasc Thorac Surg 2016;22:839-50.

**21.** Badylak SF, Freytes DO, Gilbert TW. Extracellular matrix as a biological scaffold material: structure and function. Acta Biomater 2009;5:1-13.

**22.** Badylak SF. Xenogeneic extracellular matrix as a scaffold for tissue reconstruction. Transpl Immunol 2004;12:367-77.

**23.** Mann DL, Lee RJ, Coats AJ, et al. One-year follow-up results from AUGMENT-HF: a multicenter randomized controlled clinical trial of the efficacy of left ventricular augmentation with Algisyl in the treatment of heart failure. Eur J Heart Fail 2015;18:314-25.

**24.** Zhao ZQ, Puskas JD, Xu D, et al. Improvement in cardiac function with small intestine extracellular matrix is associated with recruitment of C-kit cells, myofibroblasts, and macrophages after myocardial infarction. J Am Coll Cardiol 2010;55:1250-61.

**25.** Costanzo MR, Ivanhoe RJ, Kao A, et al. Prospective Evaluation of Elastic Restraint to Lessen the Effects of Heart Failure (PEERLESS-HF) trial. J Card Fail 2012;18:446-58.

**26.** Seghezzi G, Patel S, Ren CJ, et al. Fibroblast growth factor-2 (FGF-2) induces vascular endothelial growth factor (VEGF) expression in the endothelial cells of forming capillaries: an autocrine mechanism contributing to angiogenesis. J Cell Biol 1998;141:1659-73.

**27.** Deuse T, Peter C, Fedak PW, et al. Hepatocyte growth factor or vascular endothelial growth factor gene transfer maximizes mesenchymal stem cell-based myocardial salvage after acute myocardial infarction. Circulation 2009;120 Suppl 11:S247-54.

**28.** Okayama K, Azuma J, Dosaka N, et al. Hepatocyte growth factor reduces cardiac fibrosis by inhibiting endothelial-mesenchymal transition. Hypertension 2012;59:958-65.

**29.** Burdick JA, Mauck RL, Gorman JH 3rd, Gorman RC. Acellular biomaterials: an evolving alternative to cell-based therapies. Sci Transl Med 2013;5:176ps4.

**30.** Nguyen PK, Neofytou E, Rhee JW, Wu JC. Potential strategies to address the major clinical barriers facing stem cell regenerative therapy for cardiovascular disease: a review. JAMA Cardiol 2016;1:953-62.

**31.** Fedak PW, Bai L, Turnbull J, Ngu J, Narine K, Duff HJ. Cell therapy limits myofibroblast differentiation and structural cardiac remodeling: basic fibroblast growth factor-mediated paracrine mechanism. Circ Heart Fail 2012;5:349-56.

**32.** Vandervelde S, van Luyn MJ, Tio RA, Harmsen MC. Signaling factors in stem

cell-mediated repair of infarcted myocardium. J Mol Cell Cardiol 2005;39:363–76.

**33.** Dziki JL, Sicari BM, Wolf MT, Cramer MC, Badylak SF. Immunomodulation and mobilization of progenitor cells by extracellular matrix bio-scaffolds for volumetric muscle loss treatment. Tissue Eng Part A 2016;22:1129–39.

**34.** Smart N, Riley PR. The epicardium as a candidate for heart regeneration. Future Cardiol 2012;8:53–69.

**35.** Zhou B, Honor LB, He H, et al. Adult mouse epicardium modulates myocardial injury by secreting paracrine factors. J Clin Invest 2011;121: 1894–904.

**36.** Detillieux K, Sheikh F, Kardami E, Cattini P. Biological activities of fibroblast growth factor-2 in the adult myocardium. Cardiovasc Res 2003; 57:8–19.

**37.** Wallentin L, Becker RC, Budaj A, et al., for the PLATO Investigators. Ticagrelor versus clopidogrel in patients with acute coronary syndromes. N Engl J Med 2009;361:1045–57.

**APPENDIX** For a supplemental Methods section as well as supplemental figures and a table, please see the online version of this article.